#6092

UMIST

The University of Manchester
Institute of Science and Technology
Department of Mechanical Engineering

5th Biennial Colloquium on

Computational Fluid Dynamics

27 - 28 May 1992

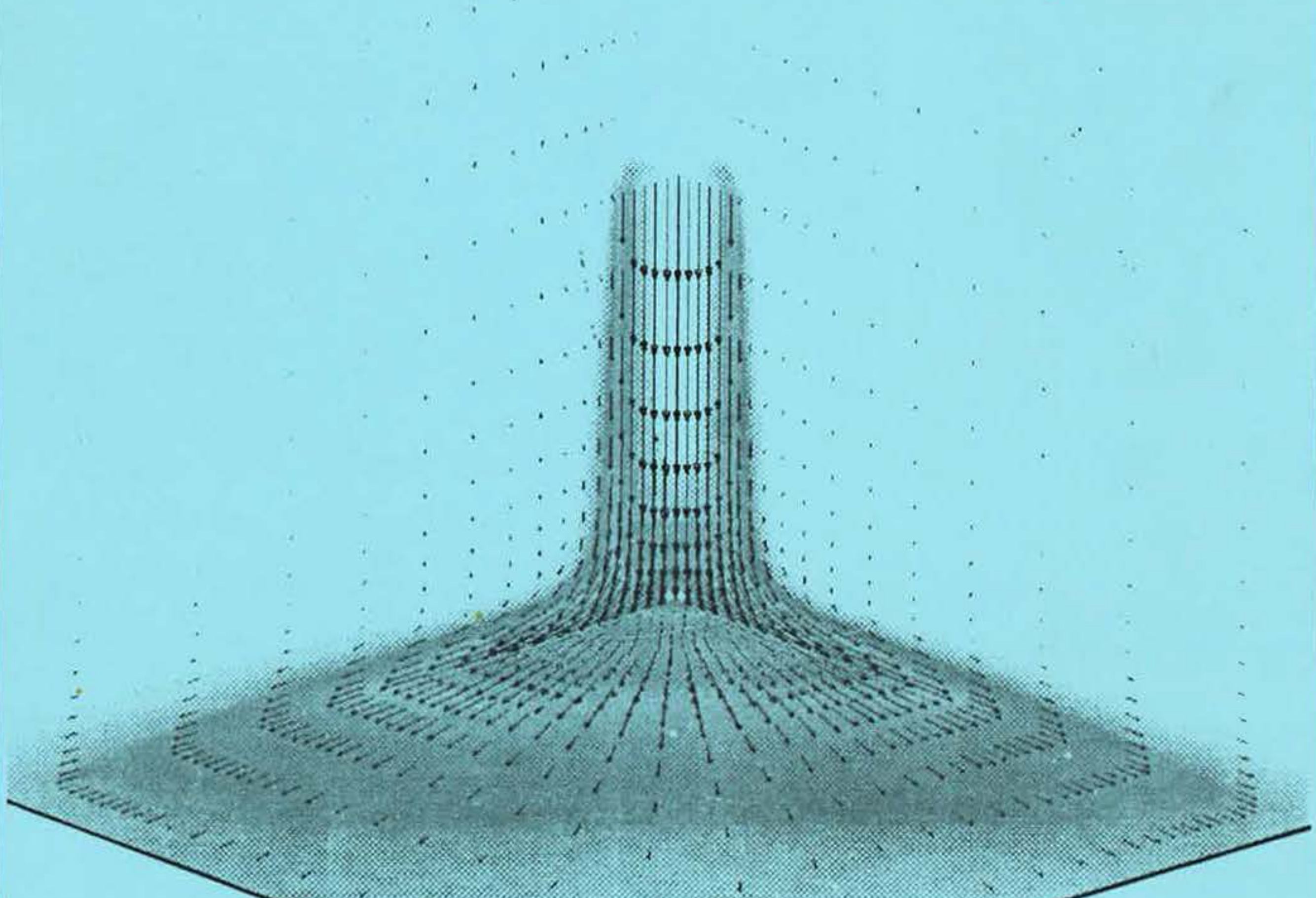

PREFACE

The booklet contains the summaries of research projects presented at the 5th Biennial CFD Colloquium held at UMIST in the period, 27-28 May 1992. The main aim of the Colloquium is to provide a broad view of ongoing research in Computational Fluid Dynamics undertaken in the Thermofluids Division of the Mechanical Engineering Department. The Colloquium is also intended as a forum for the researchers 'at the sharp end', however junior, to present the outcome of their efforts themselves to an external audience.

It is in the very nature of the Colloquium that many - indeed, the majority - of the projects are incomplete, and so firm conclusions have often not yet emerged. Nevertheless, it is our hope that listeners and readers will find that every presentation contains some useful or interesting facts.

In our desire to produce a coherent yet concise, body of information for (relatively) easy consumption, the material reported in each summary has been pruned to a small fraction of the total project. Since a *colloquium* should primarily serve as a platform for discussion, the researchers and supervisors associated with the projects presented will gladly give further details, both during and after the Colloquium. Likewise, readers of this booklet not attending the Colloquium should feel free to contact the contributors of summaries and request information in writing or in the form of referenced publications.

The large majority of projects summarised in the booklet are externally funded. It is thus appropriate that we should express our gratitude to our sponsors for their support and interest without which much of the work presented at the Colloquium would not have been done.

PROCEEDINGS OF 5TH UMIST CFD COLLOQUIUM

Turbulence Modelling - A preview
Numerical Methods - A preview

« Session 1 »

TURBULENCE MODELLING - *Fundamentals*

Paper

1.1 Second-moment modelling for strong and weak shear flows

1.2 Modelling severe inhomogeneity in near-wall turbulence

1.3 Modelling at second-moment level in rectangular ducts and riblets

1.4 A new wall-reflection treatment for the basic second-moment closure

1.5 Modelling compressibility effects on turbulent shear flows

1.6 First steps in the use of strain and vorticity invariants in two-equation modelling

1.7 Two time-level closures for compressed turbulent flows

1.8 A Lagrangian particle dispersion model accounting for time-correlation and turbulence anisotropy

1.9 Flame surface statistics by direct numerical simulation

« Session 2 »

NUMERICAL METHODS

2.1 Multigrid convergence acceleration for turbulent flow with a non-orthogonal FV algorithm

2.2 Approximation of turbulence convection with a TVD scheme

2.3 The approximation of scalar convection in unstructured grids

2.4 The adequacy of the thin shear flow equations for turbulent jets in stagnant surroundings

2.5 A new approach to overcoming pressure chequerboarding in low-order finite-element formulations of fluid flow equations

2.6 Improved wall treatments in two equation finite element modelling of turbulent flow over coarsely curved boundaries

2.7 Parallel CFD on a distributed memory machine

« Session 3 »

TURBULENCE MODELLING - *Assessment*

3.1 An ASM closure for the low-Re sublayer

3.2 Axisymmetric impinging jets: comparative performance of four turbulence models

3.3 Experiences in the use of the $\omega(\varepsilon/k)$ equation

3.4 Two equation modelling applied to drag-reducing riblets

3.5 A low-Reynolds number second moment closure for predicting by-pass transition

1 3.6 Computation of flow and heat transfer through rib-roughened channels

3.7 The calculation of separated flow with second-moment closure and low-Re turbulence models

3.8 Second-moment modelling of pre-mixed turbulent combustion

« Session 4 »

AERODYNAMIC FLOWS

4.1 Multi-element aerofoil high-lift performance at low speed and transonic flow conditions

4.2 Prediction of transonic aerofoil performance using Navier-Stokes solvers

4.3 Modelling shock/turbulent-boundary-layer interaction with second-moment closure within a pressure-velocity strategy

4.4 Predicting transonic turbulent flows over aerofoils and bumps using a cell-vertex scheme and turbulence-transport models

4.5 "EUROVAL" - A European initiative in validating CFD algorithms for turbulent aeronautical flows

4.6 Development of a computational method to predict aero-engine thrust-reversing flows

4.7 Second-moment modelling of transonic impinging jets

« Session 5 »

TWO-DIMENSIONAL FLOWS

5.1 Flow around stationary and vibrating square cylinders

5.2 Modelling of turbulent flows through port/valve assemblies

5.3 Reynolds stress modelling in engine and engine-like flows

5.4 Numerical modelling of diesel spray wall impaction phenomena - further assessment

5.5 Designing a new direct injection diesel injection system

5.6 3D diesel engine combustion simulation with EPISO procedure

« Session 6 »

THREE-DIMENSIONAL FLOWS

6.1 Computation of developing flow through a square cross-sectioned S-duct

6.2 Computation of flow through an S-bend of circular cross-section

6.3 The computation of flow and heat transfer in a sharp 180° bend

6.4 Turbulence modelling of developing flow and heat transfer in rotating ducts

6.5 Calculations of turbulent flows in multi-branch manifolds

6.6 Computation in diffusers and complex ducts with non-orthogonal FV procedure

6.7 Second-moment modelling of incompressible impinging twin jets

6.8 Three-dimensional unsteady computations of transient jet-injection into swirling cross-flow using second-moment closure

NOMENCLATURE and KEY TO ACRONYMS

AN INTRODUCTION TO TURBULENCE MODELLING AT UMIST - 1992

As at previous colloquia in the series, nearly all the research projects reported are concerned with turbulent flow. Papers in Sessions 1 and 3 involve devising or assessing new or newish models of turbulence while those in later sessions provide validation (or sometimes invalidation) of more established proposals. The long sequence of steps in a model's development implied above is an inevitable consequence of turbulence modelling being an inexact science.

The group's aim is to devise a general framework for computing turbulent flows and this requires, besides generality, flexibility and accuracy of the numerical algorithm, a mathematical representation of the turbulent motion that is also widely applicable, as regards geometry, boundary conditions and phenomena. It is the desire for generality that has driven us towards implementing second-moment closures into our software - not just for thin shear flows but recirculating and three-dimensional flows too. Present day second-moment models offer a considerably greater chance of mimicking the behaviour of a turbulent shear flow accurately than today's eddy viscosity schemes: that is conclusively established.

But what is the future potential of these two classes? Two years ago there was the sentiment that, with a new generation of "advanced" second-moment closures coming into use, eddy viscosity schemes would soon be assigned to the scrap heap - at least so far as modelling research was concerned. Today that view cannot be sustained. On the one hand the new second-moment closures have encountered some setbacks: their width of applicability - even in thin shear flows - has turned out to be narrower than had seemed likely while, on the other, the DNS data bases are providing considerable stimulus for improving 2-equation viscosity models. It is not as though, in terms of the fixed link across the Channel, one had discovered, after spending all the money, that a bridge was the better solution after all. Rather, the diversity of the strata to be pierced has given rise to some local tunnelling difficulties. In the context of second-moment closure we expect these local difficulties to be resolved in due course; certainly UMIST continues its efforts in that direction. Moreover, there is no likelihood that eddy viscosity approaches will rival the generality of a good second-moment closure; but there nevertheless seems every prospect of their being *good enough* in many cases.

Turning now to the two sessions specifically focusing on turbulence modelling issues, the first looks at new modelling proposals. There the first five presentations examine different aspects of second-moment closure - two for free shear flows and three on the question of handling near-wall effects. These reports, while addressing the same basic problem, come up with three different answers because of the different overriding constraints. It remains an important task over the next two years to unify these different viewpoints. The next two contributions deal with novel approaches to eddy viscosity models, the first on the use of strain invariants for parameterization and the second on accounting for compressibility effects in a two-time-scale model. The final two papers shift attention to the consequences of turbulent mixing so far as combustion and particle dispersion are concerned. The first, using a second-moment closure to characterize the anisotropy of the stress field, develops a physical model for the statistics of the particle field. The second employs the data base provided by a direct numerical simulation to unravel the statistical features of flames with a view to guiding the flamelet approach to combustion modelling. An increasing proportion of our turbulence modelling research in the future is likely to shift to the characterization of such reacting on two-phase flows.

Session 3, Turbulence Models - Assessment, begins with a paper that tackles the problem of providing a second-moment closure - albeit a fairly rudimentary one - that could be readily incorporated in existing software for 3-dimensional duct flows. Papers 3.2 and 3.3 both use the axisymmetric impinging jet as the vehicle for assessing turbulence models: home-grown models in the case of 3.2, a Californian import for 3.3, though with adaptations and mutations to make it better suited to the local climate. Paper 3.4 applies a low-Re k-ε model to flow over a ribleted surface while 3.5 adopts the same scheme for predicting diffusion controlled or "bypass" transition from laminar to turbulent flow in the presence of substantial external stream turbulence. In both these cases the low-Re or sublayer features of the turbulence model are vitally important to its overall success or failure. The same may be said of the flows considered in Paper 3.6: heat transfer rates in separated flows are always extremely sensitive to the turbulent transport rates in the immediate wall vicinity. Paper 3.7 presents some of the computations performed at UMIST for the Stanford collaborative exercise in turbulence modelling employing some of the same turbulence models as in Paper 3.2. Finally, Paper 3.8 also adopts a second-moment closure but as a vehicle for better characterizing the turbulent stress, heat and species fluxes in predicting turbulent reacting flows.

As in the 1990 Proceedings, there follows a tabulation of what we term 'standard turbulence models' - schemes that are repeatedly employed in the presentations or at least used as the point of departure for modelling innovations. By so doing we are enabled to keep presentations - with but one exception - to a two-page format yet still have space to discuss results. It is hoped that the inconvenience of having to refer elsewhere for the equations is outweighed by the benefits of having a compact yet informative volume.

Table 1a The Standard k~ε Eddy Viscosity Model (EVM)

$$\rho\left[\frac{2}{3}\,\delta_{ij}k - \overline{u_i u_j}\right] = \mu_t\left[\frac{\partial U_i}{\partial x_j} + \frac{\partial U_j}{\partial x_i}\right]$$

$$-\rho\overline{u_i\theta} = \frac{\mu_t}{\sigma_\Theta}\frac{\partial\Theta}{\partial x_i}$$

$$\mu_t = c_\mu\rho\,\frac{k^2}{\epsilon}$$

$$\frac{Dk}{Dt} = \frac{\partial}{\partial x_j}\left[\left[\nu + \frac{\nu_t}{\sigma_k}\frac{\partial k}{\partial x_j}\right]\right] + P + G - \epsilon$$

$$\frac{D\epsilon}{Dt} = \frac{\partial}{\partial x_j}\left[\left[\nu + \frac{\nu_t}{\sigma_\epsilon}\frac{\partial\epsilon}{\partial x_j}\right]\right] + c_{\epsilon 1}\,\frac{\epsilon}{k}\left[P + G\right] - c_{\epsilon 2}\,\frac{\epsilon^2}{k} + [YC]$$

$$P \equiv -\overline{u_i u_j}\;\partial U_i/\partial x_j; \qquad G \equiv -\beta_i\overline{u_i\theta}$$

$$YC \equiv \text{Yap Correction} = \mathrm{Max}\left(0.83\left[\frac{\ell}{\ell_e} - 1\right]\left[\frac{\ell}{\ell_e}\right]^2\frac{\epsilon^2}{k},\ 0\right]$$

c_μ	$c_{\epsilon 1}$	$c_{\epsilon 2}$	σ_Θ	σ_k	σ_ϵ
0.09	1.45	1.92	0.9	1.0	1.3

Table 1b The Standard low Reynolds no. form of k~ε EVM

As Table 1a except:

$$c_\mu = 0.09\,\exp\left[-3.4/(1 + R_t/50)^2)\right];\quad c_{\epsilon 2} = 1.92\,(1 - 0.3\,\exp - R_t^2)$$

where $R_t \equiv k^2/\nu\tilde{\epsilon}$

and, in place of the equation for ϵ,

$$\frac{D\tilde{\epsilon}}{Dt} = \frac{\partial}{\partial x_j}\left[\left[\nu + \frac{\nu_t}{\sigma_\epsilon}\right]\frac{\partial\tilde{\epsilon}}{\partial x_j}\right] + c_{\epsilon 1}\,\frac{\epsilon}{k}\left[P + G\right] - c_{\epsilon 2}\,\frac{\epsilon^2}{k} + 2\nu\nu_t\left[\frac{\partial^2 U_i}{\partial x_k\partial x_\ell}\right]^2 + YC$$

where $\epsilon \equiv \tilde{\epsilon} - 2\,\nu\,(\partial k^{\frac{1}{2}}/\partial x_j)^2$; $\mu_t = c_\mu\,\rho k^2/\tilde{\epsilon}$

The quantity $\tilde{\epsilon}$, which differs negligibly from ϵ beyond the near-wall sublayer, takes the value zero at the wall. In YC $\tilde{\epsilon}$ replaces ϵ.

Table 2: The Basic Differential Second-Moment Closure

A: Computing the Reynolds stresses

$$\underbrace{\frac{\partial \overline{u_i u_j}}{\partial t} + U_k \frac{\partial \overline{u_i u_j}}{\partial x_k}}_{C_{ij}} = d_{ij} + P_{ij} + F_{ij} + G_{ij} + \Phi_{ij} - \epsilon_{ij}$$

$$\frac{\partial \epsilon}{\partial t} + U_k \frac{\partial \epsilon}{\partial x_k} = d_\epsilon + \tfrac{1}{2} c_{\epsilon 1} \left(P_{kk} + G_{kk}\right) \frac{\epsilon}{k} - c_{\epsilon 2} \frac{\epsilon^2}{k} + YC$$

$$P_{ij} = - \left\{\overline{u_i u_k} \frac{\partial U_j}{\partial x_k} + \overline{u_j u_k} \frac{\partial U_i}{\partial x_k}\right\} \; ; \; F_{ij} = - 2\Omega_k \left\{\overline{u_j u_m}\, \epsilon_{ikm} + \overline{u_i u_m}\, \epsilon_{jkm}\right\} \; ;$$

$$G_{ij} = - \left(\overline{u_j \theta} \beta_i + \overline{u_i \theta} \beta_j\right)$$

$$\Phi_{ij} = \Phi_{ij1} + \Phi_{ij2} + \Phi_{ij3} + \left(\Phi_{ijw}\right)$$

where $\Phi_{ij1} = - c_1 \frac{\epsilon}{k} \left[\overline{u_i u_j} - \frac{1}{3} \delta_{ij} \overline{u_k u_k}\right]$

$$\Phi_{ij2} = - c_2 \left[P_{ij} - C_{ij} + F_{ij} - \frac{1}{3} \delta_{ij} \left(P_{kk} - C_{kk}\right)\right]$$

$$\Phi_{ij3} = - c_3 \left[G_{ij} - \frac{1}{3} \delta_{ij} G_{kk}\right]$$

$$\epsilon_{ij} = \frac{2}{3} \delta_{ij} \epsilon \; ; \; d_{ij} = \frac{\partial}{\partial x_k} \left[c_s \frac{k}{\epsilon} \overline{u_k u_\ell} \frac{\partial \overline{u_i u_j}}{\partial x_\ell}\right]$$

$$d_\epsilon = \frac{\partial}{\partial x_k} \left[c_\epsilon \frac{k}{\epsilon} \overline{u_k u_\ell} \frac{\partial \epsilon}{\partial x_\ell}\right]$$

$YC \equiv$ Yap correction, see Table 2

Wall Flows Only

$$\Phi_{ijw} = \Big[c_1' \frac{\epsilon}{k} \left[\overline{u_k u_m}\, n_k n_m \delta_{ij} - \frac{3}{2} \overline{u_i u_k}\, n_k n_j - \frac{3}{2} \overline{u_k u_j}\, n_k n_i\right]$$

$$+ c_2' \left[\Phi_{km2}\, n_k n_m \delta_{ij} - \frac{3}{2} \Phi_{ik2}\, n_k n_j - \frac{3}{2} \Phi_{kj2}\, n_k n_i\right]$$

$$+ c_3' \left[\Phi_{km3}\, n_k n_m \delta_{ij} - \frac{3}{2} \Phi_{ik3}\, n_k n_j - \frac{3}{2} \Phi_{kj3}\, n_k n_i\right]\Big] \frac{k^{3/2}}{c_\ell \epsilon x_n}$$

c_1	c_2	c_3	c_s	c_ϵ	$c_{\epsilon 1}$	$c_{\epsilon 2}$	c_1'	c_2'	c_3'	c_ℓ
1.8	0.6	0.5	0.22	0.18	1.44	1.92	0.5	0.3	0	2.5

Table 2 (cont'd)

B: <u>Computing the Scalar Flux and Variance</u> (Free Shear Flow Form)

$$\frac{\partial \overline{u_i\theta}}{\partial t} + \underbrace{U_k \frac{\partial \overline{u_i\theta}}{\partial x_k}}_{C_{i\theta}} = d_{i\theta} + P_{i\theta} + F_{i\theta} + G_{i\theta} + \Phi_{i\theta} - \epsilon_{i\theta}$$

$$\frac{\partial \frac{1}{2}\overline{\theta^2}}{\partial t} + U_k \frac{\partial \frac{1}{2}\overline{\theta^2}}{\partial x_k} = d_\theta + P_\theta - \epsilon_\theta$$

$$P_{i\theta} = - \overline{u_i u_k}\frac{\partial \Theta}{\partial x_k} \underbrace{- \overline{u_k\theta}\frac{\partial U_i}{\partial x_k}}_{P_{i\theta 2}} \; ; \; F_{i\theta} = - 2\Omega_k \, \overline{\theta u_m} \, \epsilon_{ikm}$$

$$G_{i\theta} = - \beta_i \frac{\overline{\theta^2}}{\Theta}$$

$$d_{i\theta} = c_\theta \frac{\partial}{\partial x_k}\left[\overline{u_\ell u_k}\frac{\partial \overline{u_i\theta}}{\partial x_k}\right]$$

$$d_\theta = c_\theta \frac{\partial}{\partial x_k}\left[\overline{u_\ell u_k}\frac{\partial \overline{\theta^2}}{\partial x_k}\right]$$

$$\Phi_{i\theta} = \Phi_{i\theta 1} + \Phi_{i\theta 2} + \Phi_{i\theta 3} + (\Phi_{i\theta w})$$

$$\Phi_{i\theta 1} = - c_{1\theta}\frac{\epsilon}{k}\overline{u_i\theta} \; ; \; \Phi_{i\theta 2} = - c_{2\theta}\,(P_{i\theta 2} - C_{i\theta} + F_{i\theta})$$

$$\Phi_{i\theta 3} = - c_{3\theta}\, G_{i\theta} \; ; \; \epsilon_{i\theta} = 0$$

$$P_\theta = - \overline{u_k\theta}\,\partial\Theta/\partial x_k \; ; \; \epsilon_\theta = \frac{1}{2}\frac{\overline{\theta^2}\epsilon}{k} R \; ; \; R^{-1} = 1.5\,(1 + A_{2\theta}) \; ;$$

$$A_{2\theta} = \frac{\overline{u_i\theta}\;\overline{u_i\theta}}{\overline{\theta^2}k}$$

$c_{1\theta}$	$c_{2\theta}$	$c_{3\theta}$	c_θ
3.0	0.5	0.5	0.18

Table 3: The New DSM Model

(For free flows only at present)

A: Computing the Reynolds stresses

As Basic Model except:

$$\Phi_{ij1} = -c_1\,\epsilon\,(a_{ij} + c_1'\,(a_{ik}\,a_{kj} - \frac{1}{3}\,\delta_{ij}\,A_2)) - \epsilon a_{ij}$$

$$\Phi_{ij2} = -0.6\,[P_{ij} - \frac{1}{3}\,\delta_{ij}\,P_{kk}] + 0.3\epsilon a_{ij}\,(P_{kk}/\epsilon)$$

$$-0.2\left\{\frac{\overline{u_k u_j}\;\overline{u_\ell u_i}}{k}\left[\frac{\partial U_k}{\partial x_\ell} + \frac{\partial U_\ell}{\partial x_k}\right] - \frac{\overline{u_\ell u_k}}{k}\left[\overline{u_i u_k}\,\frac{\partial U_j}{\partial x_\ell} + \overline{u_j u_k}\,\frac{\partial U_i}{\partial x_\ell}\right]\right\}$$

$$-r\,[A_2\,(P_{ij} - D_{ij}) + 3a_{mi}\,a_{nj}\,(P_{mn} - D_{mn})]$$

$$+t\left\{\left[\frac{7}{15} - \frac{A_2}{4}\right]\left[P_{ij} - \frac{1}{3}\,\delta_{ij}\,P_{kk}\right]\right.$$

$$+0.2\epsilon\left[a_{ij} - \frac{1}{2}\left[a_{ik}a_{kj} - \frac{1}{3}\,\delta_{ij}\,A_2\right]\right]\frac{P}{\epsilon} - 0.05a_{ij}a_{\ell k}P_{k\ell}$$

$$+0.1\left[\left[\frac{\overline{u_i u_m}}{k}\,P_{mj} + \frac{\overline{u_j u_m}}{k}\,P_{mi}\right] - \frac{2}{3}\,\delta_{ij}\,\frac{\overline{u_\ell u_m}}{k}\,P_{m\ell}\right]$$

$$+0.1\left[\frac{\overline{u_\ell u_i}\;\overline{u_k u_j}}{k^2} - \frac{1}{3}\,\delta_{ij}\,\frac{\overline{u_\ell u_m}\;\overline{u_k u_m}}{k^2}\right]\left[6D_{\ell k} + 13k\left[\frac{\partial U_\ell}{\partial x_k} + \frac{\partial U_k}{\partial x_\ell}\right]\right]$$

$$\left.+0.2\,\frac{\overline{u_\ell u_i}\;\overline{u_k u_j}}{k^2}\,(D_{\ell k} - P_{\ell k})\right\}$$

where $a_{ij} \equiv (\overline{u_i u_j} - \frac{1}{3}\,\delta_{ij}\,\overline{u_k u_k})$; $A_2 \equiv a_{ij}a_{ij}$; $A_3 \equiv a_{ij}a_{jk}a_{ki}$;

$$A \equiv 1 - \frac{9}{8}\,(A_2 - A_3)$$

and $D_{ij} \equiv -\left\{\overline{u_i u_k}\,\frac{\partial U_k}{\partial x_j} + \overline{u_j u_k}\,\frac{\partial U_k}{\partial x_i}\right\}$

$$\frac{D\epsilon}{Dt} = d_\epsilon + c_{\epsilon 1}\,\frac{\epsilon}{k}\,(P_{kk} + C_{kk}) - c_{\epsilon 2}\,\frac{\epsilon^2}{k}$$

c_1	c_1'	r	t	$c_{\epsilon 1}$	$c_{\epsilon 2}$
$3.1\,(A_2 A)^{\frac{1}{2}}$	1.2	0.6	0.0	1.0	$1.92/(1+0.7A_2^{\frac{1}{2}}A)$

Table 3 (cont'd)

B: Computing the Scalar Fluxes and Variances

As Basic Model except:

$$\Phi_{i\theta 1} = - c_{1\theta} \frac{\epsilon}{k} \left[\overline{u_i\theta}\,(1+0.6A_2)+c'_{1\theta}\, a_{ik}\,\overline{u_k\theta}+c''_{1\theta}\, a_{ik}a_{kj}\,\overline{u_j\theta}\right]-c'''_{1\theta}\, Rka_{ij}\frac{\partial\Theta}{\partial x_j}$$

$$\Phi_{i\theta 2} = 0.8\,\overline{\theta u_k}\frac{\partial U_i}{\partial x_k} - 0.2\,\overline{\theta u_k}\frac{\partial U_k}{\partial x_i} + \frac{1}{6}\frac{\epsilon}{k}\overline{\theta u_i}\frac{P_{kk}}{\epsilon} - 0.4\,\overline{\theta u_k}\, a_{i\ell}\left[\frac{\partial U_k}{\partial x_\ell}+\frac{\partial U_\ell}{\partial x_k}\right]$$

$$+ 0.1\,\overline{\theta u_k}\, a_{ik}a_{m\ell}\left[\frac{\partial U_m}{\partial x_\ell}+\frac{\partial U_\ell}{\partial x_m}\right] - 0.1\,\overline{\theta u_k}\,(a_{im}P_{mk} + 2a_{mk}P_{im})/k$$

$$+ 0.15\, a_{m\ell}\left[\frac{\partial U_k}{\partial x_\ell}+\frac{\partial U_\ell}{\partial x_k}\right](a_{mk}\,\overline{\theta u_i} - a_{mi}\,\overline{\theta u_k})$$

$$- 0.05\, a_{m\ell}\left[7a_{mk}\left[\overline{\theta u_i}\frac{\partial U_k}{\partial x_\ell} + \overline{\theta u_k}\frac{\partial U_i}{\partial x_\ell}\right] - \overline{\theta u_k}\left[a_{m\ell}\frac{\partial U_i}{\partial x_k} + a_{mk}\frac{\partial U_i}{\partial x_\ell}\right]\right]$$

$$\frac{D\epsilon_\theta}{Dt} = \left\{c_{\epsilon\theta 1}\frac{P_\theta}{\epsilon_\theta} + c'_{\epsilon\theta 1}\frac{\nu_t}{\epsilon}\left[\frac{\partial U_i}{\partial x_j}\right]^2 + \frac{c_{\epsilon\theta 3}G_{kk}}{2}\right\}\frac{\epsilon_\theta\epsilon}{Rk} - \left[c_{\epsilon\theta 2}\frac{\epsilon\epsilon_\theta}{k} + c'_{\epsilon\theta 2}\frac{\epsilon^2{}_\theta}{k}\right]$$

$$+ c_{\epsilon\theta}\frac{\partial}{\partial x_k}\left[\frac{\overline{u_k u_\ell}\,k}{\epsilon}\frac{\partial\epsilon_\theta}{\partial x_\ell}\right]$$

$c_{1\theta}$	$c'_{1\theta}$	$c''_{1\theta}$	$c'''_{1\theta}$	$c_{\epsilon\theta 1}$	$c'_{\epsilon\theta 1}$
$1.7\,(1 + 1.2\,(A_2A)^{\frac{1}{2}})R^{\frac{1}{2}}$	-0.8	1.1	$0.2A^{\frac{1}{2}}$	1.6	2.6

$c_{\epsilon\theta 2}$	$c'_{\epsilon\theta 2}$	$c_{\epsilon\theta 3}$	$c_{\epsilon\theta}$
$\frac{0.9}{1+1.1A_2A^{\frac{1}{2}}}$	$\frac{2.0}{1+1.1A_2A^{\frac{1}{2}}}$	2.6	0.18

Table 4: ASM Truncation

- Stress transport is eliminated by the approximations:

$$\frac{D\,\overline{u_i u_j}}{Dt} = \frac{\overline{u_i u_j}}{k}\frac{Dk}{Dt}$$

$$d_{ij} = \frac{\overline{u_i u_j}}{k}\, d_k$$

- Heat transfer studies employing an ASM approximation for the stress field have adopted the GGDH form for $\overline{u_i u_j}$:

$$\overline{u_i \theta} = 0.35\,\frac{k}{\epsilon}\,\overline{u_i u_k}\,\frac{\partial \Theta}{\partial x_k}$$

NUMERICAL ISSUES - A Preview

The foregoing Preview conveyed a flavour of the central importance of turbulence closure to predictive realism, of present limitations and of directions taken at UMIST towards removing model weaknesses, principally within the framework of second-moment closure. In the context of industrial aerodynamics, the most sophisticated turbulence model is of little utility, however, without a flexible, accurate and economical numerical vehicle that allows the model's application to the type of complex conditions for which it was ultimately constructed. From this standpoint, the turbulence model may be viewed as a component - an ingredient, in the interactive mix making up a useful computational algorithm for turbulent flows.

With attention focused here on numerical issues, it may be said that the ability of CFD procedure to provide accurate predictions rests on four main issues:

(1) the geometric flexibility of the numerical mesh;
(2) the accuracy of the approximation techniques used to transform the differential equations to algebraic equivalents;
(3) the density of the mesh used for supporting the solution; and
(4) the efficiency of the numerical algorithm.

Until 1989, efforts at UMIST directed at geometric flexibility, in the context of finite-volume methods, had taken the route of designing *orthogonal*-mesh algorithms. While these offered considerably greater flexibility than Cartesian variants - and are still being used in 2D as well as 3D applications - the requirement of orthogonality is constraining and leads to undesirable node depletion and enrichment, divorced from physical rationale. This has motivated efforts to develop general *non-orthogonal structured* as well as *unstructured* methods, and their associated capabilities are conveyed superficially in the figure below.

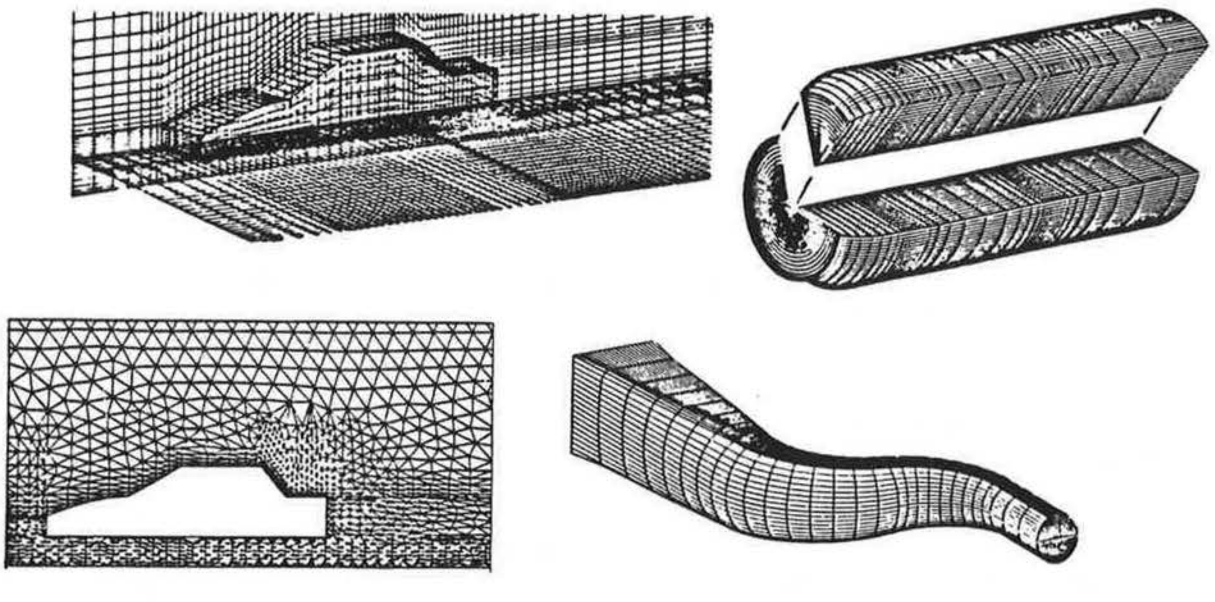

Mesh types used within UMIST's finite-volume solution strategies

Several summaries to follow deal with applications, both 2D and 3D, which have made use of the enhanced geometric capabilities developed mainly over the past two years. Variants of the structured-grid method have been applied in areas as diverse as shock-boundary-layer interaction in transonic jet/afterbody geometries and curved transition ducts in which the cross-sectional area changes from a rectangular to a circular shape. Unstructured-grid methods have been used, principally, for modelling viscous aerodynamic flows around aerofoils, but efforts are underway to construct a pressure-based unstructured-grid algorithm for incompressible 2D and 3D flows.

Limitations under (2), (3) and (4) above can be reduced, in principle, to insignificant levels with the availability of unlimited computing resources. Approximation and resolution errors decline as the supporting grid is refined. However, the penalties arising from such refinement are, first, an obvious linear increase in memory and, second, a less obvious non-linear increase in CPU requirement. Typically, the latter rises in proportion to (number of nodes)$^{2.5}$, which means that a doubling of node density in any one spatial direction increases CPU time by a factor of order 100 in three-dimensional flow. The clear message is then that an accurate approximation in a practical environment must involve a combination of accurate numerical schemes combined with convergence-acceleration techniques and increased execution efficiencies by exploiting modern hardware architectures. A number of Summaries contain in this booklet demonstrate awareness of the importance of all three issues and document related contributions.

As regards approximation techniques, the large majority of computations performed with all types of turbulence closure use higher-order approximations for convection. Unbounded as well as bounded variants of upstream-weighted quadratic interpolation are routinely employed in 2D and 3D computations, whether the mesh is rectilinear, curved-orthogonal or non-orthogonal. Increasingly, TVD or MUSCL-type schemes come into play, particularly in efforts to solve the turbulence-model equations to an accuracy consistent with that of the aerodynamic set. TVD schemes are also used at UMIST for solving mixed hyperbolic/ elliptic problems arising in transonic viscous flows.

Improvements in computational efficiency are pursued along two routes, one algorithmic and the other exploiting advanced hardware architectures. The former involves extensive explorations within the multigrid area, and current capabilities at UMIST extend to turbulent flows computed with non-orthogonal grids and second-moment closure as well to 3D geometries. In the latter area, parallel computing is being explored, both for general incompressible viscous flow and transonic flow. The main approach adopted rests on domain decomposition, in which sub-domains are allocated to associated processors (Transputers), all working in parallel. A Summary to follows demonstrates that close to linear scalability can be achieved if careful attention is paid to problem size relative to the number of collaborating processors

Looking ahead towards 1994, we see major numerical strides being made in the area of modelling 3D flows, both compressible and incompressible, with unstructured grids, combining virtually unlimited flexibility with adaptivity, multigrid acceleration and, last but not least, the advanced turbulence-modelling strategies emerging from the hierarchical sequence or 'pipeline' of 'simple' attached and separated flow for which the models have been validated with the aid of standard numerical solvers.

« Session 1 »

TURBULENCE MODELLING - *Fundamentals*

« Session 1 »

TURBULENCE MODELLING - *Fundamentals*

SECOND-MOMENT MODELLING FOR STRONG AND WEAK SHEAR FLOWS

Research Worker: A.M. El Baz
Supervisor: B.E. Launder
Sponsor: DRA (Fort Halstead)

1. BACKGROUND

Data on grid-turbulence decay by Le Penven & Gence [1] have shown that, if velocity fluctuations in two orthogonal directions are greater than the average ('hamburger' turbulence), the decay pattern is quite different from that when only one component is greater than the average ('frankfurter' turbulence) for the same mean degree of anisotropy. The second-moment closures in use at UMIST do not capture this feature. The aim of the present study has been to devise a pressure-strain model that captured the effects noted while at the same time retaining at least as satisfactory performance in other shear flows.

2. APPROACH

To achieve the different decay patterns observed in experiment requires that, in approximating the process ϕ_{ij}, use be made of the third invariant of the Reynolds stress: $A_3 = a_{ij}a_{jk}a_{ki}$, or (which is more convenient) the flatness parameter $A = 1 - 9/8\ (A_2 - A_3)$. The form emerging from the optimization was

$$\begin{aligned}\phi_{ij1} &= -\ 2.5A^{1/2}\ (1 - A)^{1/2}\ \epsilon\ a_{ij} \\ &+ 6.5(A_2A)^{1/2}\epsilon\left(a_{ik}a_{kj} - \frac{1}{3}\ \delta_{ij}\ A_2\right) - \epsilon\ a_{ij}\end{aligned} \tag{1}$$

which, as seen from Fig 1, does much better in capturing the stress decay than UMIST's "New" model.

However, with this change, agreement with the homogeneous shear flow experiments [2,3] is very poor, Fig 2. Working within the cubic model, reasonable agreement with experiment could only be restored by including non-zero values for the 't' coefficient. In fact the form we have chosen is:

$$r = 0;\ t = 5.6\sqrt{A_2}$$

Figure 2 indicates that with this choice agreement is nearly as good as with the standard values $r = 0.6;\ t = 0$.

With ϕ_{ij1} and ϕ_{ij2} fixed the model has been applied to a range of inhomogeneous shear flows. For the plane mixing layer, Fig 3, the predicted shear stress profile is as satisfactory as with the standard model (though $\overline{v_2}$ is somewhat too low), while for the far axisymmetric wake, where shear effects are weak, only the present proposal shows a decay exponent for the turbulent velocities of - 2/3 (a value with which experiments and analysis concur), Fig 4.

REFERENCES

1. Le Penven, L., Gence, J.N. and Comte-Bellot, G., 'On the approach to isotropy of homogeneous turbulence: effect of the partition of kinetic energy among the velocity components', in Frontiers in Fluid Mech., ed. S.H. Davies and J.L. Lumley, Springer, 1985.

2. Champagne, F.H., Harris, V.G. and Corrsin, S.C., 'Experiments on nearly homogeneous turbulent shear flow', J. Fluid Mech., 41, 81, 1970.

3. Harris, V.G., Graham, J.A.H. and Corrsin, S.C., 'Further experiments in nearly homogeneous shear flow', J. Fluid Mech., 81, 657, 1977.

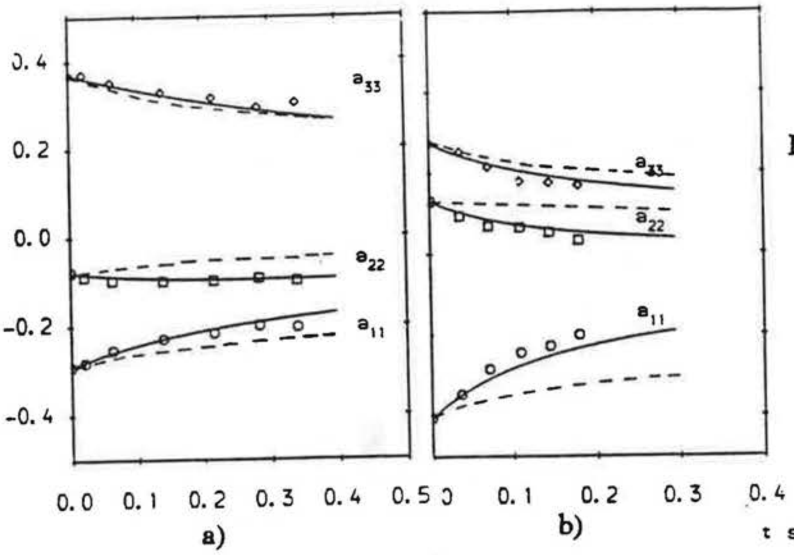

Fig 1 Decaying anisotropic turbulence
a) $A_3 > 0$
b) $A_3 < 0$
--- Standard model;
___ equation (1)
Symbols are experiments

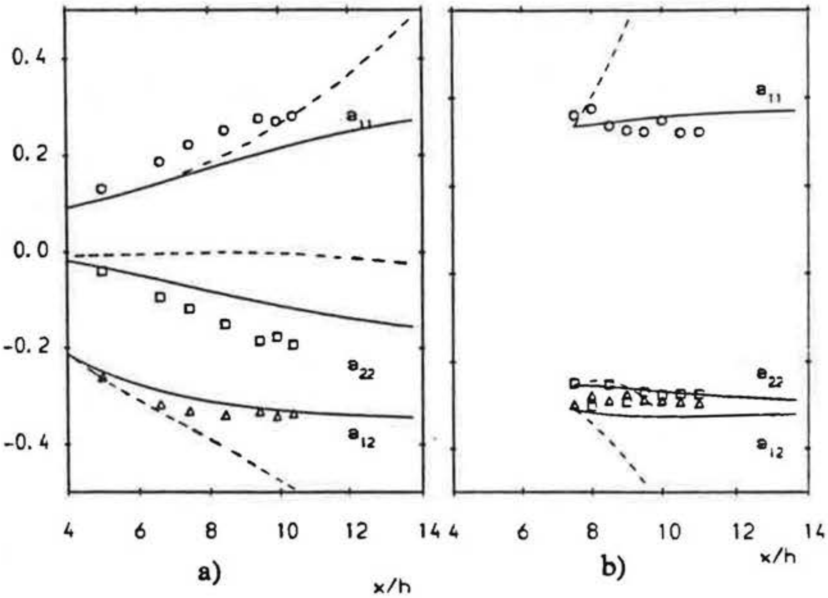

Fig 2 Homogeneous shear flows
a) local equilibrium case
b) high strain case
--- $r = 0.6$, $t = 0$;
___ $r = 0$, $t = 5.6\sqrt{A_2}$

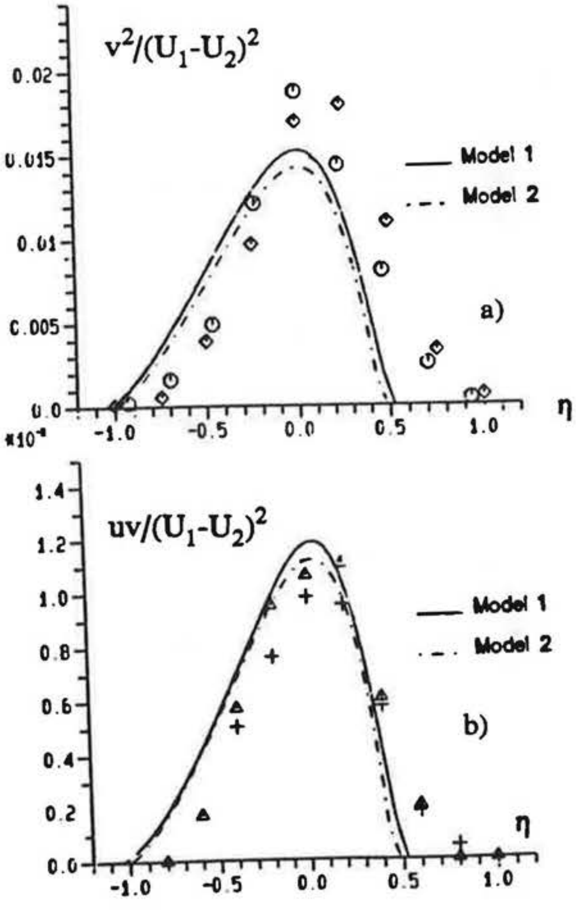

Fig 3 Plane mixing layer

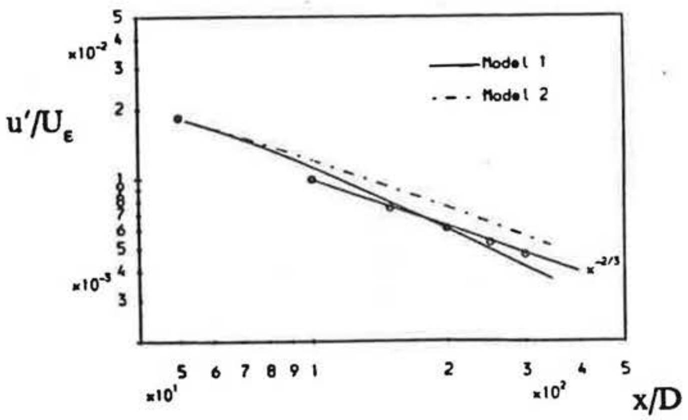

Fig 4 Far axisymmetric wake: decay of streamwise fluctuations